2012-5-8

# Terahertz Surface Plasmon Polaritons on Freestanding Multi-Walled Carbon Nanotube Aerogel Sheets

T. D. Nguyen, *et al.*

# Terahertz surface plasmon polaritons on freestanding multi-walled carbon nanotube aerogel sheets

**T. D. Nguyen,[1] S. Liu,[2] M. D. Lima,[3] S. Fang,[3] R. H. Baughman,[3] A. Nahata,[2] and Z. V. Vardeny[1,*]**

[1]*Department of Physics, University of Utah, Salt Lake City, UT 84112, USA*
[2]*Department of Electrical and Computer Engineering, University of Utah, Salt Lake City, UT 84112, USA*
[3]*Alan G. MacDiarmid NanoTech Institute, University of Texas at Dallas, Richardson, TX 75083 USA*
**val@physics.utah.edu*

**Abstract:** We demonstrate that multi-walled carbon nanotubes (MWCNTs) are capable of supporting surface plasmon-polaritons (SPPs) at terahertz (THz) frequencies. To achieve this, we fabricated sub-100 μm-thick freestanding and highly oriented multi-walled carbon nanotube (MWCNT) aerogel sheets. Utilizing terahertz time-domain spectroscopy, we measured the complex index of refraction of the sheets for two orthogonal nanotube orientations. We found that the MWCNT sheets exhibit highly anisotropic THz polarization behavior. Based on the extracted dielectric properties of the medium, which show that it exhibits metallic behavior in the THz spectral range, we investigated the existence and propagation of SPPs by studying the resonantly enhanced transmission through periodic MWCNT hole arrays. We found that carbon nanotubes support SPP excitations that propagate along the tubes, but highly suppress these surface waves in the direction perpendicular to the nanotubes.



**OCIS codes:** (160.4236) Nanomaterials; (240.6680) Surface plasmons; (050.1220) Apertures; (260.3090) Infrared, far.

## References and links

1. M. A. McCarthy, B. Liu, E. P. Donoghue, I. Kravchenko, D. Y. Kim, F. So, and A. G. Rinzler, "Low-voltage, low-power, organic light-emitting transistors for active matrix displays," Science **332**(6029), 570–573 (2011).
2. Z. Wu, Z. Chen, X. Du, J. M. Logan, J. Sippel, M. Nikolou, K. Kamaras, J. R. Reynolds, D. B. Tanner, A. F. Hebard, and A. G. Rinzler, "Transparent, conductive carbon nanotube films," Science **305**(5688), 1273–1276 (2004).
3. M. Zhang, S. Fang, A. A. Zakhidov, S. B. Lee, A. E. Aliev, C. D. Williams, K. R. Atkinson, and R. H. Baughman, "Strong, transparent, multifunctional, carbon nanotube sheets," Science **309**(5738), 1215–1219 (2005).
4. T.-I. Jeon, K.-J. Kim, C. Kang, I. H. Maeng, J.-H. Son, K. H. An, J. Y. Lee, and Y. H. Lee, "Optical and electrical properties of preferentially anisotropic single-walled carbon-nanotube films in terahertz region," J. Appl. Phys. **95**(10), 5736–5740 (2004).
5. T.-I. Jeon, K.-J. Kim, C. Kang, S.-J. Oh, J.-H. Son, K. H. An, D. J. Bae, and Y. H. Lee, "Terahertz conductivity of anisotropic single walled carbon nanotube films," Appl. Phys. Lett. **80**(18), 3403–3405 (2002).
6. M. Liang, Z. Wu, L. Chen, L. Song, P. Ajayan, and H. Xin, "Terahertz characterization of single-walled carbon nanotube and graphene on-substrate thin films," IEEE Trans. Microw. Theory Tech. **59**(10), 2719–2725 (2011).
7. A. Katsounaros, M. Mann, M. Naftaly, K. Z. Rajab, Y. Hao, and W. I. Milne, "Terahertz time-domain spectroscopy characterization of vertically aligned carbon nanotube films," Carbon **50**(3), 939–942 (2012).
8. J. Kyoung, E. Y. Jang, M. D. Lima, H.-R. Park, R. O. Robles, X. Lepró, Y. H. Kim, R. H. Baughman, and D.-S. Kim, "A reel-wound carbon nanotube polarizer for terahertz frequencies," Nano Lett. **11**(10), 4227–4231 (2011).
9. L. Ren, C. L. Pint, L. G. Booshehri, W. D. Rice, X. Wang, D. J. Hilton, K. Takeya, I. Kawayama, M. Tonouchi, R. H. Hauge, and J. Kono, "Carbon nanotube terahertz polarizer," Nano Lett. **9**(7), 2610–2613 (2009).
10. W. A. deHeer, W. S. Bacsa, A. Châtelain, T. Gerfin, R. Humphrey-Baker, L. Forro, and D. Ugarte, "Aligned carbon nanotube films: production and optical and electronic properties," Science **268**(5212), 845–847 (1995).
11. M. F. Islam, D. E. Milkie, C. L. Kane, A. G. Yodh, and J. M. Kikkawa, "Direct measurement of the polarized optical absorption cross section of single-wall carbon nanotubes," Phys. Rev. Lett. **93**(3), 037404 (2004).
12. H. H. Gommans, J. W. Alldredge, H. Tashiro, J. Park, J. Magnuson, and A. G. Rinzler, "Fibers of aligned single-walled carbon nanotubes: Polarized Raman spectroscopy," J. Appl. Phys. **88**(5), 2509–2514 (2000).

#165301 - $15.00 USD Received 22 Mar 2012; revised 4 May 2012; accepted 5 May 2012; published 8 May 2012

13. T. W. Ebbesen, H. J. Lezec, H. F. Ghaemi, T. Thio, and P. A. Wolff, "Extraordinary optical transmission through sub-wavelength hole arrays," Nature **391**(6668), 667–669 (1998).
14. T. Matsui, A. Agrawal, A. Nahata, and Z. V. Vardeny, "Transmission resonances through aperiodic arrays of subwavelength apertures," Nature **446**(7135), 517–521 (2007).
15. A. Agrawal, Z. V. Vardeny, and A. Nahata, "Engineering the dielectric function of plasmonic lattices," Opt. Express **16**(13), 9601–9613 (2008).
16. T. Matsui, Z. V. Vardeny, A. Agrawal, A. Nahata, and R. Menon, "Resonantly-enhanced transmission through a periodic array of subwavelength apertures in heavily-doped conducting polymer films," Appl. Phys. Lett. **88**(7), 071101 (2006).
17. F. J. García de Abajo, J. J. Sáenz, I. Campillo, and J. S. Dolado, "Site and lattice resonances in metallic hole arrays," Opt. Express **14**(1), 7–18 (2006).

## 1. Introduction

Carbon nanotubes (CNTs) have attracted significant attention because of their unique electrical, optical and mechanical properties [1–3]. Recently, there has been growing interest in studying the physical properties of highly aligned carbon nanotube sheets [3–9]. A unique aspect of these materials is the fact that this structure has high electrical and optical anisotropy that results from their large aspect ratio, making CNTs a nearly ideal quasi-one-dimensional system. This anisotropy manifests itself in numerous different ways. For example, ellipsometry measurements at optical frequencies have demonstrated the highly anisotropic nature of the dielectric constants and conductivities of aligned CNTs [9,10]. The polarized absorption of single-walled carbon nanotubes (SWCNTs) have been reported, which has allowed for the determination of the nematic order parameters of the sample [11]. The polarization-dependent Raman scattering measurements of substantially aligned SWCNT fibers showed dramatic reduction of the Raman intensities in all spectra for the perpendicular excitation compared to those in parallel excitation, while the relative intensities of the radial and the tangential modes remained unchanged [12]. In measurements of the anisotropic conductivity of SWCNT films [4–6] and multi-walled CNT (MWCNT) films [7], it was found that it follows a Drude-like behavior for lossy metals at THz frequency. However in both materials, the samples were prepared on glass slides or Si wafers. This ambient environment may affect the optical and electrical properties of the materials.

In this submission, we characterize the THz optical spectra of *free standing* MWCNT films using terahertz time-domain spectroscopy (THz-TDS) for incident radiation polarized parallel and perpendicular to the nanotube axis. While there is strong anisotropy in the extracted dielectric constants, the medium exhibits metallic behavior for both orientations, which is a necessary condition for supporting surface plasmon-polaritons (SPPs). Based on this finding, we fabricated an array of subwavelength apertures in 25 μm and 60 μm thick sheets of MWCNTs. In the case of the thinner CNT sheet, we observed enhanced optical transmission [13,14] only when the incident radiation was polarized parallel to the CNT axis. However, for the slightly thicker sheet, we did not observe enhanced transmission with either orientation. This suggests that absorption within the apertures is significant in this material.

## 2. Experimental details

A MWCNT 'forest' was synthesized by catalytic chemical vapor deposition [3]. The CNT sheet was drawn from a sidewall of the forest on steel washers with an inner diameter of ~2 cm. Multiple forest-drawn MWCNT films can be made by stacking together parallel sheets so that the orientation of the nanotubes are parallel to each other. The CNT sheet thickness was determined by counting the number of layers. We studied two different MWCNT sheets: a 25 μm thick sheet having 12 layers and a 60 μm thick sheet composed of 30 layers. From the thickness and measured areal sheet density, the volumetric density was calculated to be very light, ~0.0015 g/cm$^3$. In Fig. 1(a), we show a photograph of a portion of an aperture array fabricated in the 30-layer, 60 μm thick freestanding CNT sheet drawn on top of a steel washer. For the CNT hole array (HA) fabrication, we used an excimer laser to mill holes in the CNT sheets. The array consisted of 0.65 mm diameter circular holes fabricated on a square lattice with a periodicity of 1.2 mm.

#165301 - $15.00 USD Received 22 Mar 2012; revised 4 May 2012; accepted 5 May 2012; published 8 May 2012

We used a THz-TDS setup (shown in Fig. 1(b)) for measuring the optical transmission spectra, t(ω) of the unperforated and perforated MWCNT films, where the THz frequency ν = ω/2π. Photoconductive devices were utilized for both emission and coherent detection of the THz field. Two off-axis paraboloidal mirrors were used to collect and collimate the vertically polarized THz beam from the emitter and focus the beam to the detector. The samples were attached to a solid metal plate with a 2 cm x 2 cm opening that is significantly larger than the THz beam size, and placed in the path of the collimated THz beam. The detected transient photocurrent, PC(τ) was recorded as a function of the translation stage path that determined the time delay, τ between the 'pump' beam that hits the emitter and the 'probe' beam that arrives at the detector. PC(τ) was subsequently Fourier transformed and normalized to a reference transmission, yielding both the electric field transmission *magnitude and phase*, t(ω) in the range ~0.1 THz to 0.5 THz. The resulting Fourier transformed data may be described by the relation:

$$t(\omega) = |t(\omega)| \exp[i\varphi(\omega)] = \frac{E_{\text{transmitted}}(\omega)}{E_{\text{incident}}(\omega)}. \quad (1)$$

In this expression $E_{incident}$ and $E_{transmitted}$ are the incident and transmitted THz fields, respectively, and |t(ω)| and φ(ω) are the magnitude and phase of the amplitude transmission coefficients, respectively. The THz-TDS technique is unique in that it allows for a direct measurement of the transient THz electric field transmitted through the structures, yielding both amplitude and phase information. From such spectra both real and imaginary components of the refractive index, n(ω) can be directly obtained without the need for Kramers-Kronig transformations, where somewhat arbitrary assumptions about asymptotic behavior are typically made.

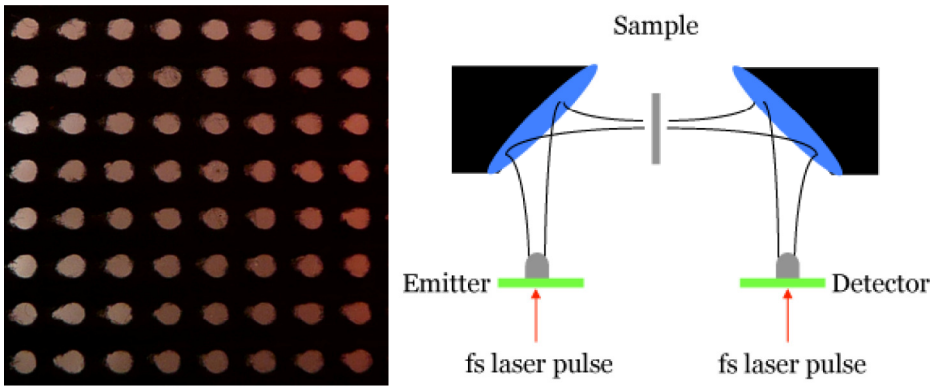


(a) (b)

Fig. 1. (a) Photograph of the perforated carbon nanotube sheet with 30 CNT layers. The circular apertures have a diameter, d, of 0.65 mm and a periodic spacing, a, of 1.2 mm arranged in a square lattice. (b) Schematic drawing of the THz TDS experimental geometry.

### 3. Results and discussion

In order to study SPP propagation on perforated MWCNT sheets, we first need to fully characterize the complex dielectric properties of the unperforated MWCNT sheets. In Fig. 2(a) we show the measured THz time-domain waveforms transmitted through a 25 μm MWCNT sheet, where the nanotubes are aligned parallel or perpendicular to the incident THz polarization (hereafter, these will be referred to as 'parallel' and 'perpendicular'). For reference purposes, we also show the time-domain waveform associated with the incident THz beam. It is apparent that the transmission properties are strongly dependent on the orientation of the nanotubes. This polarization dependence can be more clearly seen when the transient photocurrent in Fig. 2(a) is Fourier transformed to yield the normalized amplitude

#165301 - $15.00 USD Received 22 Mar 2012; revised 4 May 2012; accepted 5 May 2012; published 8 May 2012

and phase spectra in the frequency domain (see Eq. (1)), as shown in Figs. 2(b) and 2(d), respectively. Using these two orientations, we observe an extinction ratio ($T_{\perp}/T_{//}$) of ~2. Similar THz polarization behavior in CNT sheets has been observed previously by several groups [4–9].

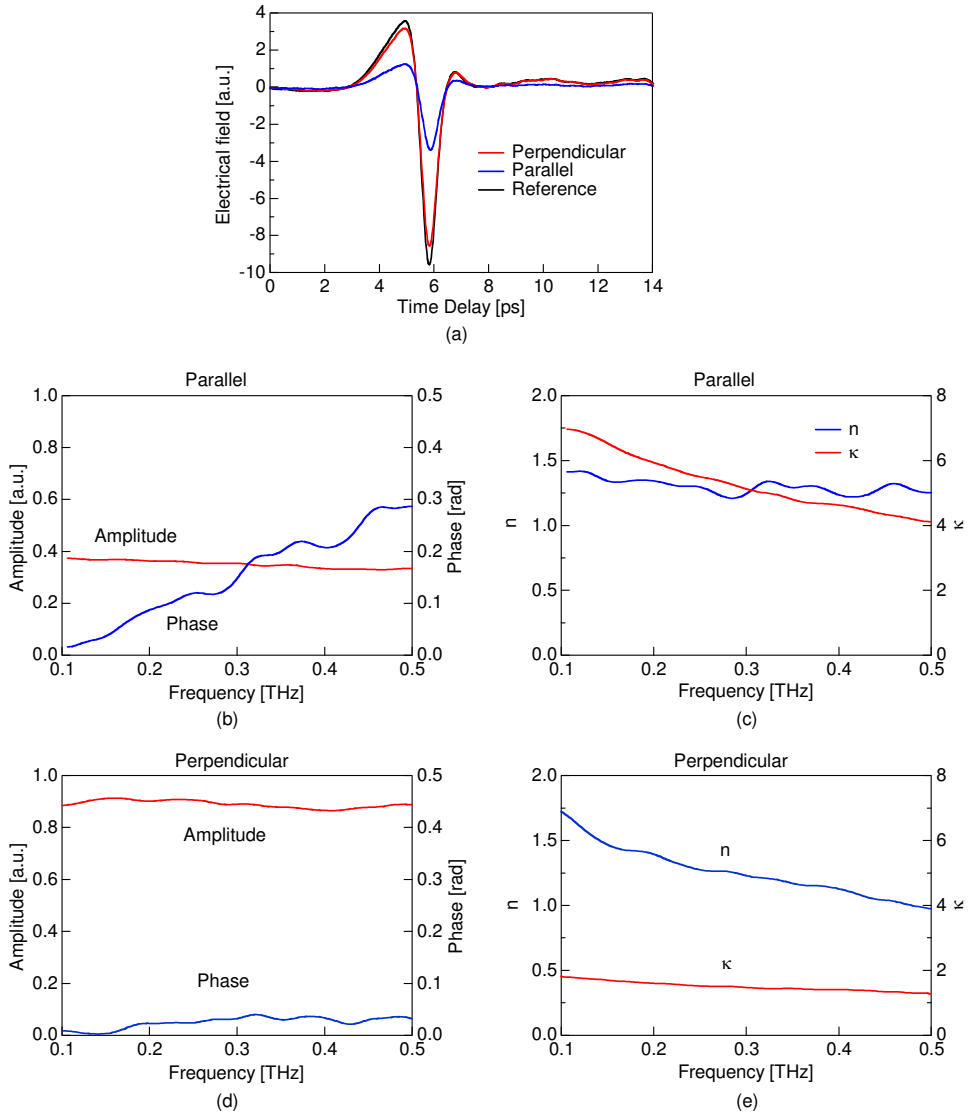


Fig. 2. Transmission and dielectric properties of MWCNT sheets. (a) THz time-domain waveforms of the transmission through a 25 μm MWCNT sheet for parallel and perpendicular orientations. The transmission spectra (b,d) and complex refractive index components, n and κ (c,e) in the parallel (b,c) and perpendicular (d,e) orientations, respectively, as obtained from (a). Note the scale difference between n and κ.

From the amplitude and phase information of the transmission, we can readily calculate the frequency-dependent complex index of refraction, n and κ, as shown in Figs. 2(c) and 2(e). While the real component, n of the refraction index for the two nanotube orientations is similar, there is a large difference in the imaginary index of refraction, κ, which is related to the absorption coefficient. The frequency dependent absorption coefficient is given by the relation $\alpha(\nu) = 2\pi\nu\kappa/c$, where the electric field decay is given by $\exp[-\alpha(\nu)d]$), ν is the THz

#165301 - $15.00 USD Received 22 Mar 2012; revised 4 May 2012; accepted 5 May 2012; published 8 May 2012

frequency and c is the speed of light in vacuum. Based on the data in Figs. 2(c) and 2(e), the absorption coefficient is smaller at lower photon energy, which is in agreement with previous studies [4–6]. In order for a medium to support SPPs, the sign of the real component of the dielectric constant, $\varepsilon_r = n^2 - \kappa^2$, must be negative. Based on the data in Figs. 2(c) and 2(e), $\varepsilon_r$ is negative for both orientations over the entire THz spectral range studied here, demonstrating that SPPs can be supported in principle.

It is well known [13,14] that gratings having periodic or aperiodic order may be used to compensate for the momentum mismatch between the incident light and SPP dispersion. In the case of subwavelength hole arrays, this results in SPP-induced enhancement of the transmission at several resonant frequencies. With this in mind, we fabricated periodic hole arrays with periodicity of 1.2 mm and circular hole diameter of 0.65 mm in the nanotube sheets via laser ablation. In Fig. 3(a), we show the measured THz waveforms transmitted through a CNT hole array using a CNT sheet with a thickness of 25 μm and with the nanotubes aligned parallel to the incident THz polarization. The transmission spectrum shows that only ~50% of the THz field is transmitted.

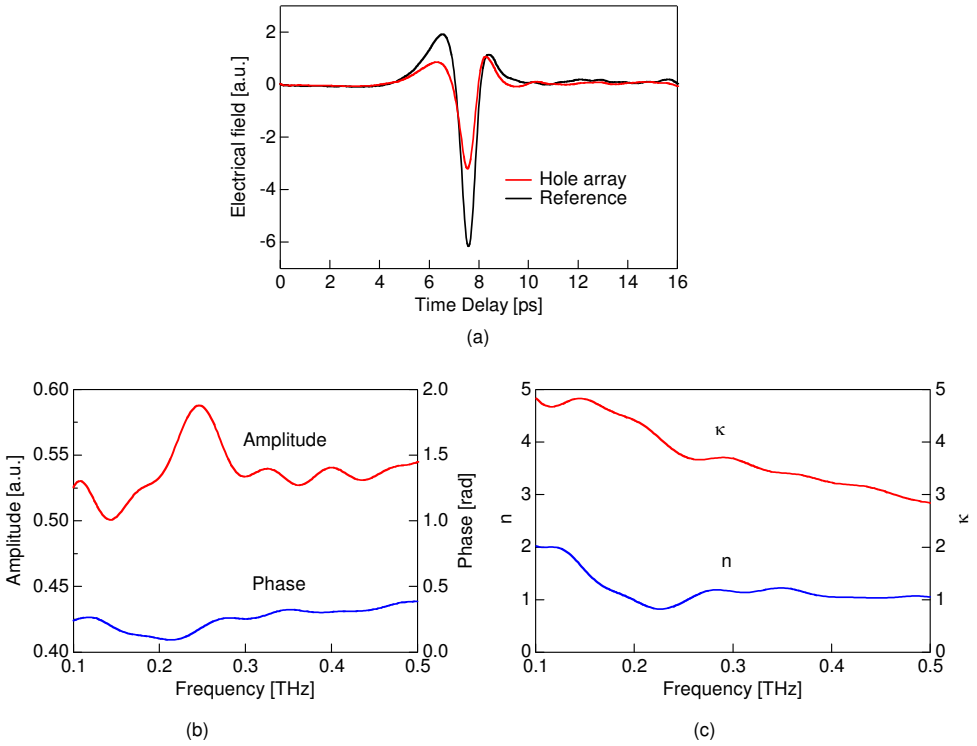


Fig. 3. (a) THz time-domain waveforms measured after transmission through a MWCNT hole array with 0.65 mm diameter holes and 1.2 mm periodicity in a *parallel* orientation, along with the reference. (b) Amplitude and phase spectra obtained from (a). (c) Calculated complex refractive index spectra, n and κ obtained from (b).

In Fig. 3(b), we show the corresponding amplitude and phase spectra. Though weak, there is a clear resonance in the transmission spectra at ~0.25 THz. In order to explain the location of this resonance, we note that the anti-resonance (AR) frequencies (as opposed to the resonance frequencies) can be found directly from the spatial Fourier transform of the real space aperture geometry [14]. In the case of a periodic array, the AR frequencies are given analytically by [13]:

#165301 - $15.00 USD Received 22 Mar 2012; revised 4 May 2012; accepted 5 May 2012; published 8 May 2012

$$\nu_{AR} = \frac{c}{P n_{SPP}} \sqrt{i^2 + j^2}, \tag{2}$$

where

$$n_{SPP} = \left[ \frac{\varepsilon_m \varepsilon_d}{\varepsilon_m + \varepsilon_d} \right]^{1/2}. \tag{3}$$

In these equations, $n_{SPP}$ is the effective refractive index for the propagating SPP, $\varepsilon_m$ and $\varepsilon_d$ are the complex dielectric constants of the array medium and the adjacent dielectric media, respectively, P is the aperture periodicity, and i and j are integers that index the resonance order. Using the data in Fig. 2(c), we find that $n_{SPP} \cong n_{air} \approx 1.015$. From Eq. (2), we calculate the lowest order AR frequency, corresponding to $i = \pm 1$ and $j = 0$, to occur at a frequency $\nu_{AR} \approx 0.25$ THz. The associated transmission resonance peak appears at a frequency that is just slightly smaller than this value. Although a clear AR is not apparent in Fig. 3(b), the computed value is in good agreement with our observations.

The transmission resonance further demonstrates that SPP excitations do exist and propagate on the one-dimensional nanotube structure. In contrast to the resonantly enhanced light transmission in a stainless steel structure, the transmission peak here is much weaker because of the greater THz absorption [15,16]. Furthermore, the transmission peak is quite broad and does not clearly show an anti-resonance dip at frequencies higher than the resonant frequency at ~0.25 THz peak. This indicates, more generally, that carbon nanotubes are lossy at THz frequencies, in agreement with the conclusions of Katsounaros *et al*. [6]. The effective imaginary component, $\kappa$ of the structure in Fig. 3(c) clearly shows that the absorption at 0.25 THz is smaller than at other frequencies, corresponding to a larger transmission. Nevertheless, the observed resonance transmission of around 8% is encouraging, when taking into account the very low density of the MWCNT sheet ($0.0015 mg/cm^3$). We also examined the electric field transmission properties of the MWCNT HA with perpendicular orientation (not shown). We found that the resonantly enhanced light transmission through the CNT sheet *does not occur* in this case. The probable reasons are: (i) very low conductivity along this direction over this frequency range (see Figs. 2(d) and 2(e)); and (ii) SPPs do not exist for directions orthogonal to the nanotube axis, because it is a nearly ideal quasi-one-dimensional system.

Up to this point, we have only examined the 25 μm thick MWCNT sheet. In Fig. 4(a) we show the strong THz transmission anisotropy for a 60 μm MWCNT sheet. In this case, the extinction ratio ($T_{\perp}/T_{//}$) is nearly 40, which is more than an order of magnitude larger than the value obtained with the 25μm MWCNT sheet, and in good agreement with the literature [7,8]. Based on the high absorption for the parallel orientation (see Fig. 4(a)) we fabricated an array of subwavelength hole apertures with parameters identical to those for the 25 μm thick film. However, in this case we did not observe any resonantly enhanced transmission in either orientations, as can be seen from the transmission spectra shown in Fig. 4(b). This indicates that although the THz absorption from the film is high because of the high conductivity, the energy launched from the apertures in the form of SPP waves is probably reabsorbed in the thick MWCNT material. This places a practical limit on the thickness of MWCNT sheets for plasmonics applications. Nevertheless it is clearly seen that the transmission spectrum of the perforated film in the parallel geometry increases for $\nu > \sim 0.2$ THz, indicating that the individual holes still act as transmission enhancers [14], even though there is no SPP interference between the holes, which is necessary to yield transmission resonances [15]. In order to clarify this point, in Fig. 4(c) we plot the transmission spectra for the parallel orientation in Fig. 4(b) along with the calculated (normalized) transmission expected for a single aperture [14,17]. The good agreement between the data and model calculation confirms that the apertures act as individual transmission enhancers, but do not communicate with other apertures via launched SPPs, because of the large attenuation that hampers SPP propagation on the film surfaces.

#165301 - $15.00 USD Received 22 Mar 2012; revised 4 May 2012; accepted 5 May 2012; published 8 May 2012

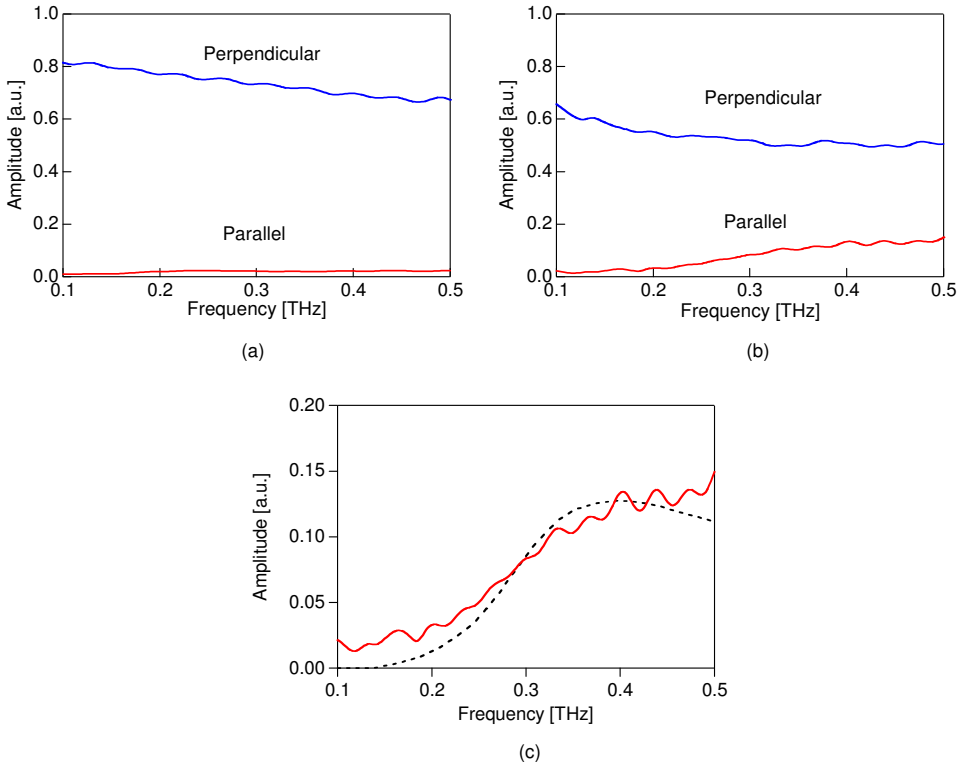


Fig. 4. THz transmission spectrum from (a) a 60 µm thick unperforated MWCNT sheet, and (b) the same film perforated with a periodic hole array with 0.65 mm diameter apertures and 1.2 mm periodicity on a square lattice, for both parallel (red) (blue) orientations. (c) The transmission spectrum for the hole array (parallel orientation from (b)) [red line] and the calculated normalized transmission for a single aperture (dashed black line) plotted in an extended scale.

## 4. Conclusions

We fabricated sub 100 µm-thick freestanding and highly oriented MWCNT sheets using the catalytic chemical vapor deposition method. Using THz-TDS we measured the complex index of refraction spectrum of the sheets for two orthogonal nanotube orientations. We found that the thick CNT sheet shows highly anisotropic THz polarization behavior with extinction ratio values of ~40. We investigated the existence and propagation of SPP excitations at THz frequencies by studying the resonantly enhanced transmission spectrum through periodic aperture arrays fabricated on the MWCNT sheets. We found that CNTs support SPP propagation along the tubes. However, no SPP-related enhanced transmission was detected in the perpendicular direction. Furthermore we found that the *resonant* enhanced transmission is absent in aperture arrays fabricated on a thick MWCNT sheet, although the individual apertures still act as transmission enhancers. These somewhat contradictory results can be explained by the strong re-absorption of the SPP excitations on the CNT sheet that prevents SPP propagation along the surfaces.

## Acknowledgments

This work was supported by the NSF MRSEC program at the University of Utah under grant # DMR 1121252.

#165301 - $15.00 USD Received 22 Mar 2012; revised 4 May 2012; accepted 5 May 2012; published 8 May 2012